

A new method for CSF shunt patency assessment

Marek Swoboda, Matias G. Hochman, Jenna S Fritz, Mark E. Mattiucci, Frederick J Fritz

NeuroDx Development LLC

CSF shunts employed to treat hydrocephalus patients malfunction frequently, usually by obstruction, but the symptoms of shunt failure are non-specific [5]. Diagnosis of shunt malfunction by conventional means is difficult, expensive, and associated with risks to the patient (exposure to radiation from CT Scans, risk of infection from shunt taps and radionuclide testing) [5]. A new diagnostic method to assess shunt patency which combines a non-invasive CSF flow generator and a thermal CSF flow meter has emerged. The presented method estimates the hydraulic resistance of the shunt system in addition to measuring shunt flow. The authors believe that this new technique will increase sensitivity and specificity in the diagnosis of shunt patency compare to existing methods. The method was tested in vitro in 16 popular shunt systems, the results show that it can differentiate between patent, partially obstructed and fully obstructed shunts in 15 out of 16 shunt systems. This work opens a new possibility of shunt patency assessment using a non-invasive, inexpensive and easy to use procedure.

keywords: CSF shunt, CSF shunt patency, hydrocephalus, CSF shunt obstruction, Thermal dilution device

1. Background. Approximately 69,000 people are diagnosed with hydrocephalus each year in the United States [1]. The most common treatment for hydrocephalus is diversion of CSF from the brain ventricles to the peritoneal cavity by means of a permanent prosthetic shunt. However, the one-year failure rate of implanted shunts has been estimated to be approximately 40% [2,3], and the mean period to failure is typically only five to ten years [4]. Obstruction, usually from tissue in-growth or clots at the inflow catheter, is overwhelmingly the greatest cause of shunt failure [2, 5-8]. Shunt failure can rapidly progress to life-threatening elevation in intracranial pressure, so revision surgery and replacement of the blocked catheter is indicated. However, symptoms of shunt obstruction

(headache, nausea, lethargy) are non-specific, and it has been calculated that three false alarms are seen at the emergency department for every true shunt malfunction [5]. Computed Tomography (CT) remains the standard approach for differentiating an obstructed shunt from a false alarm [5, 9], however this technique produces a static image, resulting in the need for serial imaging to confirm CSF build-up. Repeat radiation exposures of these patients (often children) from repeat CT scans is a recognized and growing concern among neurosurgeons [10]. Radionuclide shunt flow testing and shunt taps are invasive and pose a risk of infection, so they are not used to investigate every headache. New technologies under development are complex (ultrasound tracking of bubbles),

lacking in precision (FLIR) or require implantation (implanted thermal flow technologies) and have not reached the clinic.

Thermodilution methods were developed [12] to facilitate rapid and non-invasive detection of cerebrospinal fluid flow through subcutaneous shunts where obstruction is suspected. Those methods employ thermal dilution technology - detecting a transcutaneous change in temperature as cooled cerebrospinal fluid flows through the subcutaneous portion of a shunt. An example of such method is shown in Figure 1. A thermal stimulus (ice) is applied to the skin surface. It cools down neighboring tissue. The temperature differential generated within tissue volume changes the amount of heat ΔQ within shunt tubing. With CSF mass flow the ΔQ is transferred downstream where it causes tissue temperature change, this temperature change is registered on the skin surface by an array of thermistors. The presence or absence of CSF flow is interpreted by a change in temperature on the skin surface (Figure 1).

1.1 Clinical utility of Thermal CSF Flow Detection

The clinical utility of thermal CSF flow

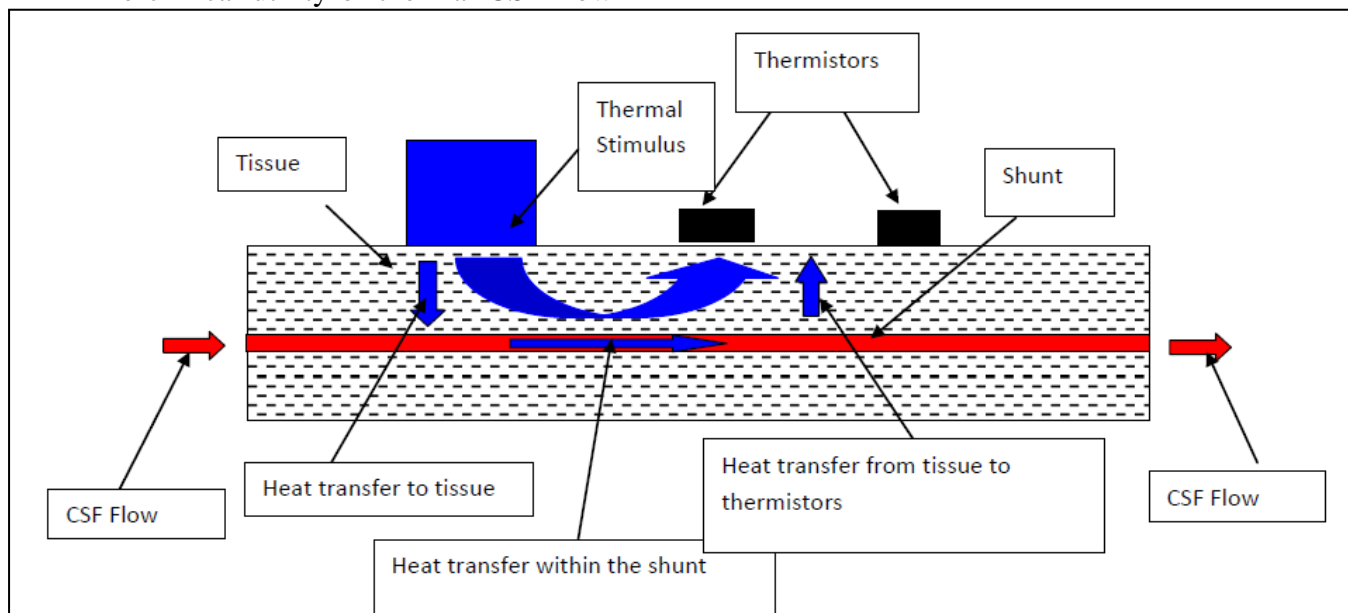


Figure 1 A generic representation of a thermodilution method for CSF flow detection in shunt tubing implanted under the skin surface. Heat transfer linked to CSF mass flow generates thermal response downstream the thermal stimulus.

detection is limited by intermittent CSF flow and partial occlusion. The FDA 510(k) application for one thermal CSF flow detector [23] demonstrated that the detection device exhibits 100% accuracy in detecting lack of flow through a subcutaneous shunt in an animal model [11]. However, the clinical utility of the device (or any single-point flow test) in identifying shunt obstruction is based on the assumption that CSF flows constantly through patent (unobstructed) shunts. This premise has been insufficiently supported through prior characterization of CSF flow in asymptomatic patients – whether CSF flows constantly or intermittently through “normal” shunts was not known.

A study of 100 asymptomatic and symptomatic pediatric hydrocephalus patients at Boston Children’s Hospital [12] found that patients with patent shunts exhibited CSF flow during only 54% of tests. This result is almost identical to that previously reported using radionuclide tracing, in which only 53% of subjects with patent shunts exhibited CSF flow at the time of testing [13]. These results strongly suggest that CSF flows only intermittently (approximately 50% of the time) through patent shunts [14]. Intermittent CSF flow can therefore

cause false positive (“obstructed”) test results, and limits the diagnostic specificity of flow detectors such as dilution thermal CSF flow detection device.

Perhaps more importantly, this study identified ten symptomatic patients with thermodilution results of “Flow” but CT scans which indicated enlarged ventricles (evidence of elevated ICP and an obstructed shunt). These patients went on to shunt revision surgery during which it was determined that their shunts were only partially occluded and were flowing. Bench tests described below show that when shunts are over 95% blocked (see table 1.), a build-up of CSF and consequent rise in ICP can cause CSF to flow within a normal range of flow rates even though the ICP is dangerously elevated. Thermodilution or radionuclide methods will detect this flow even though this flow, due to shunt's high hydraulic resistance to outflow, is insufficient to resolve the pathology. Partial occlusion causes false negative test results and limits the diagnostic sensitivity of thermal CSF flow detection.

The occurrence of intermittent flow in patent shunts, and low but measurable flow in partially-occluded shunts necessitates more than a method for detecting the presence or absence of CSF flow through a shunt at the time of testing. What is needed is a tool for measuring the resistance to flow through a shunt (i.e. its level of occlusion), in order to differentiate clinically-relevant obstruction from physiological (temporary) CSF stasis. By measuring resistance one can easily assess blockage level and flow capacity of the shunt.

1.2. Flow generator

This need led to the development of a hand-held, non-invasive CSF flow generator which “interrogates” the shunt by delivering specific vibration pulses to the shunt valve dome. This generates controlled, reproducible CSF flow through patent, but not occluded or partially occluded shunts. This temporary

increase in flow can then be detected via thermal dilution.

The flow generator has been designed as a simple vibrator vibrating at 60Hz for 60 seconds. The acceleration delivered to the dome was approximately from 0.6 to 1 g (5.9 to 9.8 m/s²). The vibrator consists of a plastic foot with a miniature DC motor mounted on it. The DC motor is outfitted with a counterweight. The device’s vibration frequency, duration and duty cycle are controlled by an electronic circuit.

In some cases, in order to scale the flow rate, vibration with less than 100% duty cycle was used (pulsing rather than continuous vibration). Our experiments show that duty cycle doesn't change the principle features of the system but decreases the flow rate proportionally to the % of the duty cycle. A prototype of the flow generator is shown in figure 2.



Figure 2 Flow generator is a simple mechanical vibrator which gently vibrates the shunt valve dome through the scalp tissue. It uses a specific frequency and vibration pattern to maximize pumping efficiency and protect ventricles from excessive suction.

1.3. Problem statement

The flow generator can be integrated into the thermodilution diagnostic procedure only if it meets certain functional and clinical requirements. To answer the technical validity

and clinical utility question, one has to experimentally evaluate the following hypotheses:

Hypothesis 1. The flow generator is capable of generating robust flow in patent (but not occluded) shunts in a broad and representative range of commercially available shunt valves.

Hypothesis 2. The combined flow generator plus the thermal CSF flow detection method can reliably differentiate between patent flow and partially occluded flow.

Hypothesis 3. Vibrational CSF flow generation is safe – it generates limited CSF drainage, it does not generate strong ventricular suction and it does not damage shunt valves nor change the setting of programmable valves.

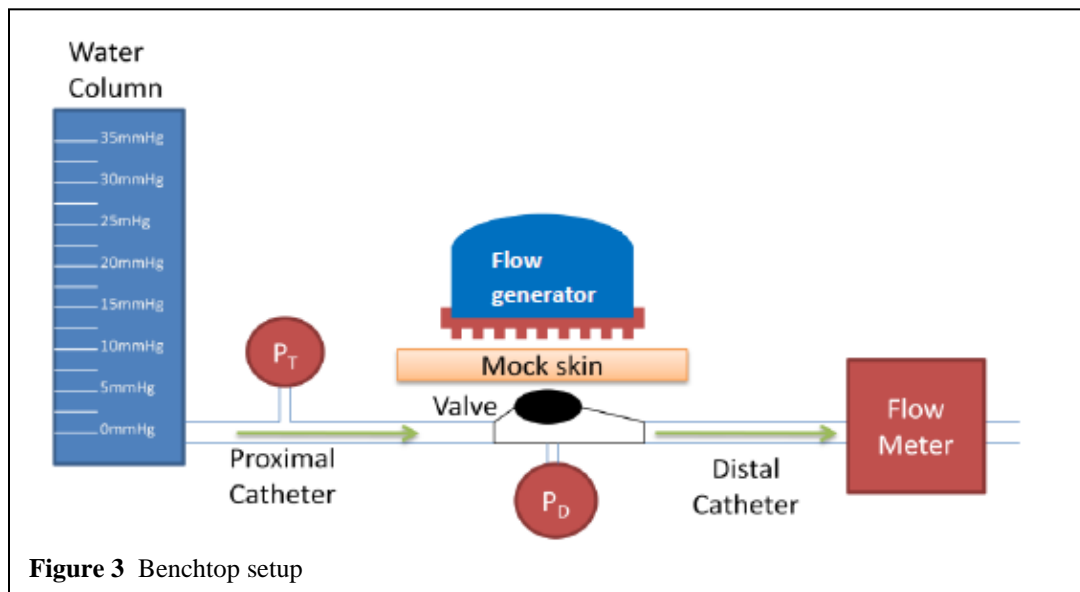
2. Materials and methods

Experimental setup and conditions

In our bench top experiment, we used a ventricle simulator, ventricular shunt catheter, shunt valve, distal catheter, Medtronic CSF drainage system and an optical flow meter (drop counter). The system for flow rate studies is shown in figure 3.

In the thermal portion of this study, we also used a thermal skin simulator and a thermal CSF flow detector thermal dilution device.

We tested responses to flow generation with a drop counter flow meter and subsequently with the thermal CSF flow detector. When experimenting with thermodilution system, the drop counter flow meter and the Medtronic drainage system were replaced by a thermally active mock skin with shunt tubing embedded in it (thermal skin simulator). The thermodilution sensor was placed on the thermally active mock skin over the distal portion of the shunt tubing emulating regular clinical application. This setup simulated thermal behavior of human skin with implanted shunt tubing, and allowed us to replicate the physics of the thermal dilution method of assessing CSF flow. The resistance introduced by the thermal skin simulator was similar to the Medtronic drainage system and negligible in the order of 0.1 [mmHg/ml/h]. Proximal and distal resistances were simulated by needle resistors placed in series with shunt tubing. Needle resistors simulate occlusion of shunt tubing by narrowing the lumen. A short explanation of this approach is offered below.



Note: Illustration of proximal occlusion and hydraulic resistances.

Shunt occlusion is a complex process and the authors are not trying to describe it in this paper. For illustrative purposes, we decided to show a specific example of occlusion which can help the reader visualize resistance values used in our experiments. In this example, we utilized a 20cm of 1 mm ID shunt tubing (it can represent a section of the proximal catheters). The original cross-sectional area of the shunt corresponds to 100% patency. Decreased (occluded) cross-sectional areas are described as % of the original area of the lumen. We assume that the shunt gets occluded by deposits on the inner walls of the tubing and that the deposits are uniformly distributed over the inner surface of the tubing, resulting in uniform narrowing of the lumen. Corresponding hydraulic resistances are shown in figure 4 and table 1.

The table 1 shows several **examples** of patency and corresponding hydraulic resistances. The numbers in the table follow the model described above - 20cm of 1mm ID tubing with 7 different levels of occlusion

expressed as % of the original 1 mm ID lumen. One can see that when the lumen gets down to 10% of its original cross-sectional area (90%

Patency %	Resistance [ml/h]
100	.017
60	.045
30	.17
10	1.6
5.7	5.1
4.8	7.2
4	10.6

Table 1. The % occlusion and corresponding hydraulic occlusions for a uniformly occluded 20 cm 1mm ID shunt catheter.

occluded), the hydraulic resistance of the 20 cm 1 mm OD tubing reaches 1.6 [mmHg/ml/h]. Hydraulic resistance rises rapidly as occlusion levels exceed 90%. For lower occlusion levels (e.g. 30% patent or 70% occluded) the resulting hydraulic resistance is negligible.

2.1 Flow generation in patent and occluded shunts

To test how flow rate is modulated by proximal resistance, we used the setup shown in

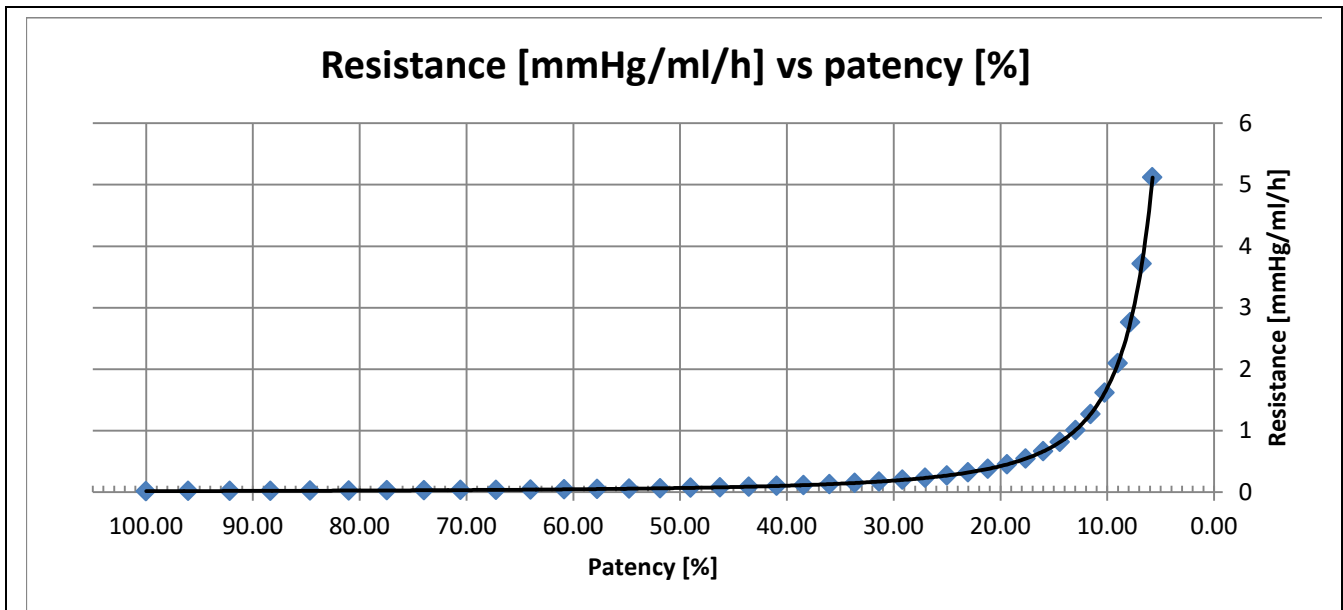


Figure. 4 Shows the relationship between hydraulic resistance of the 20 cm shunt tubing (1 mm ID) and its patency calculated as a percentage of cross-sectional area of the original (patent) lumen of the tubing. We assume, in this model, that the lumen is uniformly occluded, decreasing cross-sectional area of the shunt lumen. This is only for illustrative purposes; the occlusion mechanisms are many and can occur in different places of the proximal catheter.

figure 3. The resistances of the proximal catheter were simulated by calibrated needle resistors placed in series with proximal and distal catheters. The distal resistance was kept constant at a low level of approximately 0.1 [mmHg/ml/h]. The ICP was kept at ~ 5cm of H₂O and the abdominal pressure at 0. Partial proximal occlusion was simulated by a needle resistor of 4 [mmHg/ml/h], comparable to approximately 95% occlusion.

2.1.1 Flow rate vs. Distal and Proximal patency

To test two dimensional proximal and distal resistance flow dependency, both distal and proximal obstructions were simulated by needle resistors. We decided to choose one common shunt system (Medtronic Strata with Siphon Control) to study its behavior in two dimensional parameter space namely how the CSF flow generated by the flow generator changes for various combinations of proximal and distal resistances. The distal and proximal resistances were varied from 0 to 4 [mmHg/ml/h] on the proximal side and from 0 to 3 [mmHg/ml/h] on the distal side.

2.1.2 Abdominal pressure - flow relationship

In order to answer how the difference between ICP and ABP values influences CSF flow generated by the flow generator, we used the same setup as in 2.1.1 but for each combination of proximal and distal resistances, we varied the pressure difference between the proximal and distal ends. The pressures were 10, 5, 0, -5, -10 [cmH₂O]. This experiment emulated changes to ICP from positive to negative (e.g. changes from supine to sitting position) or buildup of the abdominal pressure.

2.2. Differentiating between patent, partially obstructed and totally obstructed shunts using the thermal CSF flow detection device (proximal patency-the most common case in pediatric hydrocephalus)

In this part of the study, we designed a simple test to assess how the method differentiates between patent, partially patent and obstructed shunts, using the same setup as in 2.1. Six shunt valves were tested, the Medtronic Strata and Delta, the Sophysa Polaris, the Integra Ultra VS neonate and Integra DP and the Codman Hakim. The proximal hydraulic resistance was varied between 0.1 (patent), 4 (partial occlusion) and infinity (completely occluded shunt) [mmHg/ml/h]. Resistances were simulated by needle resistors connected in series with catheter tubing. Patent and partially occluded shunts were tested under two different initial conditions – flowing (at 3 to 5 ml/h) or non-flowing. ICP was adjusted to achieve these flow rates. Patent shunts were tested at 0 cmH₂O (no flow) and approximately 5cmH₂O (flowing). Partially occluded shunts were tested at 10 cmH₂O (no flow) and approximately 18 cmH₂O (to simulate flow with elevated ICP). Totally occluded shunts were tested at 18 cmH₂O. The abdominal pressure was set at 0. The flow rate generated by the flow generator was tested with a calibrated optical flow meter (drop counter). The flow meter counts drops inside the Medtronic drainage system via optical means, thus it doesn't introduce any additional resistance.

2.2.1. Assessing the impact of skin thickness and hair.

This experiment replicated the procedure from 2.2.1 but instead of testing occluded and partially occluded systems, we focused on patent shunts. Several shunt systems were tested with two levels of skin thickness and hair (4 cases, namely thin, medium and thick skin and medium skin with hair). Synthetic hair was used.

2.3. Safety

Assessing pressures inside the dome.

In this experiment we used Strata with Siphon Control valves. To test pressure

amplitude inside the dome, we inserted a rigid catheter through the flat bottom of the dome and measured pressure using a standard medical pressure transducer EDWARDS PX272 . A special care was given to minimize the dead volume in the junction between the valve and the pressure transducer. Frequency of the flow generator was 60 Hz. Pre-stress force applied by the flow generator foot to the valve dome was approximately 1.27 Newtons. The valve dome was covered by artificial skin (SynDaver) 5mm thick to mimic mechanical properties of the human scalp tissue.

Assessing pressure at the tip of the ventricular catheter.

The same type of transducer was used to measure P_T pressure at the end of the ventricular catheter (see figure 3). Pressures generated by manual shunt pumping (1 sec push and quick

release) were compared with pressures generated by the flow generator vibrating at 60Hz for 60 seconds.

3. Results

3. 1. Hypothesis 1. The flow generator is capable of generating robust flow in patent (but not occluded) shunts in a broad and representative range of commercially available shunt valves. Figure 5. shows flow rate increase due to vibrational flow generation for three popular valves including one with a siphon control device (MDT Strata).

The flow generator does generate a robust, temporary increase in CSF flow rate in patent shunts but only very limited flow in partially occluded shunts and no flow in occluded shunts.

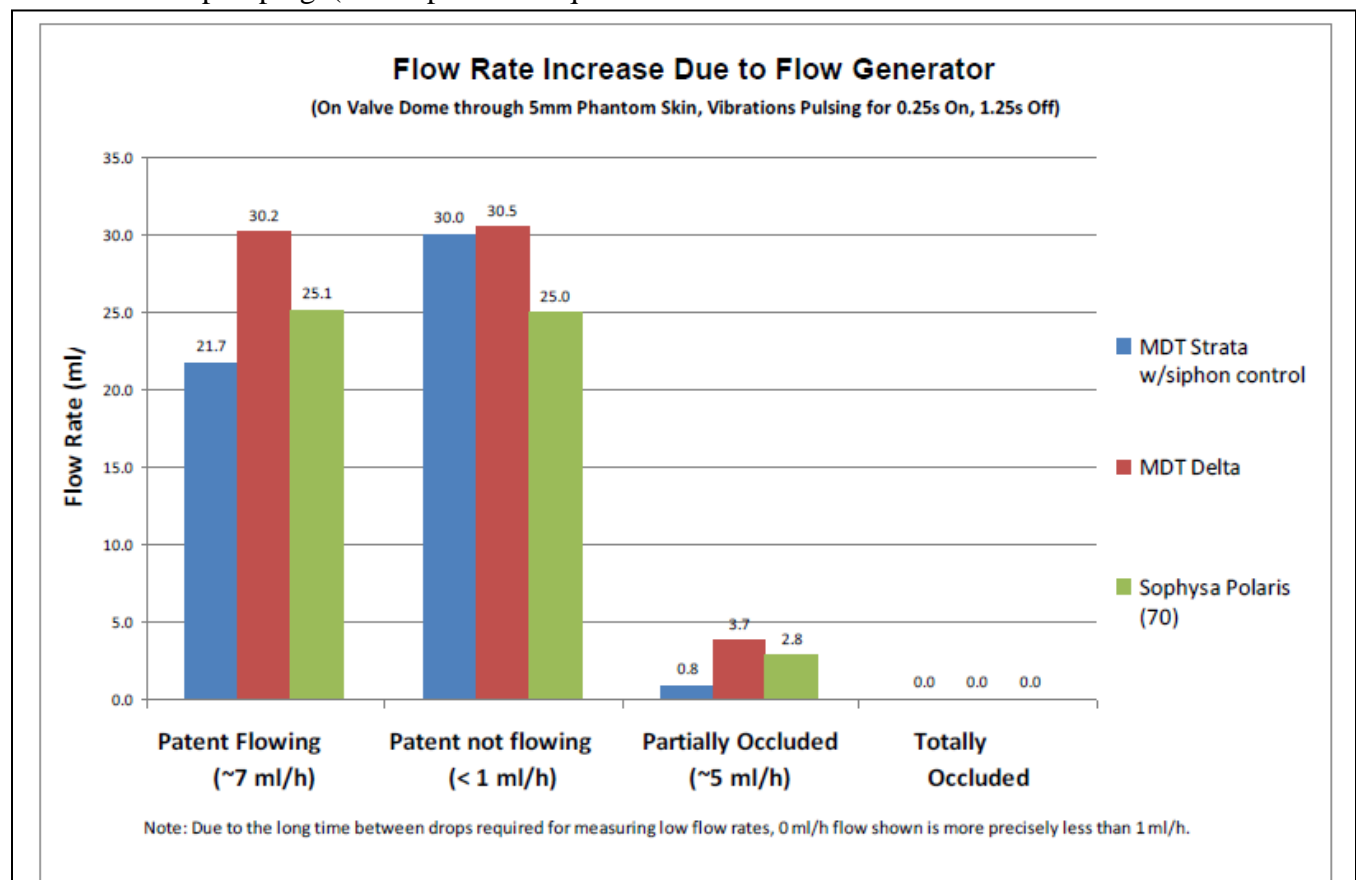


Figure 5 Change in flow in three shunt systems treated with Flow generator. Two initial conditions: natural flow and no flow (<1ml/h). Partial occlusion was represented by a needle resistor of 4 [mmHg/ml/h]

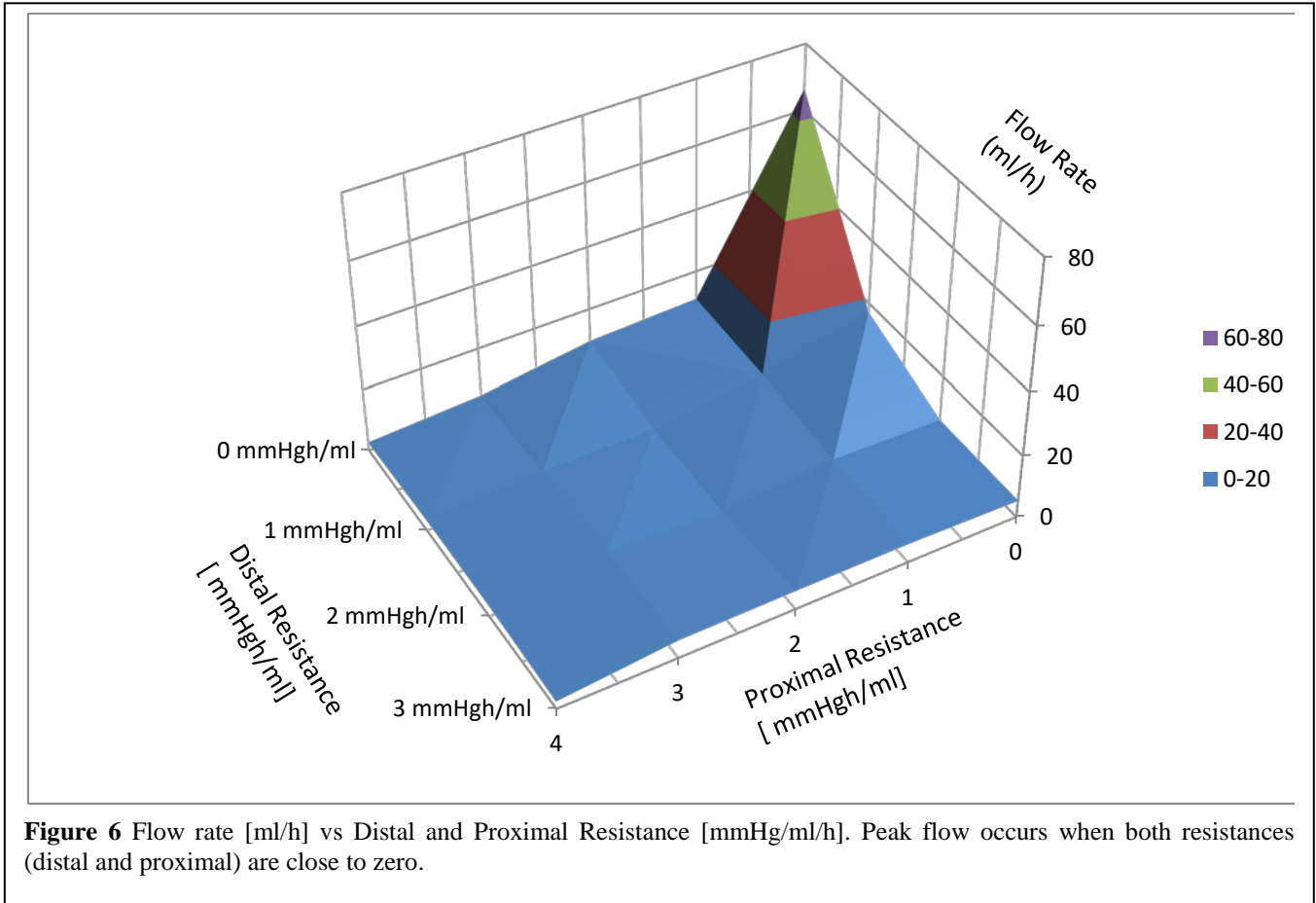
3.1.1. Flow rate vs Distal and Proximal resistance

Highest flow rates were registered at lowest proximal and distal resistance values (see figure 6).

low single digits values which can be below the thermal LOD (Limit Of Detection) of the thermal CSF flow detector.

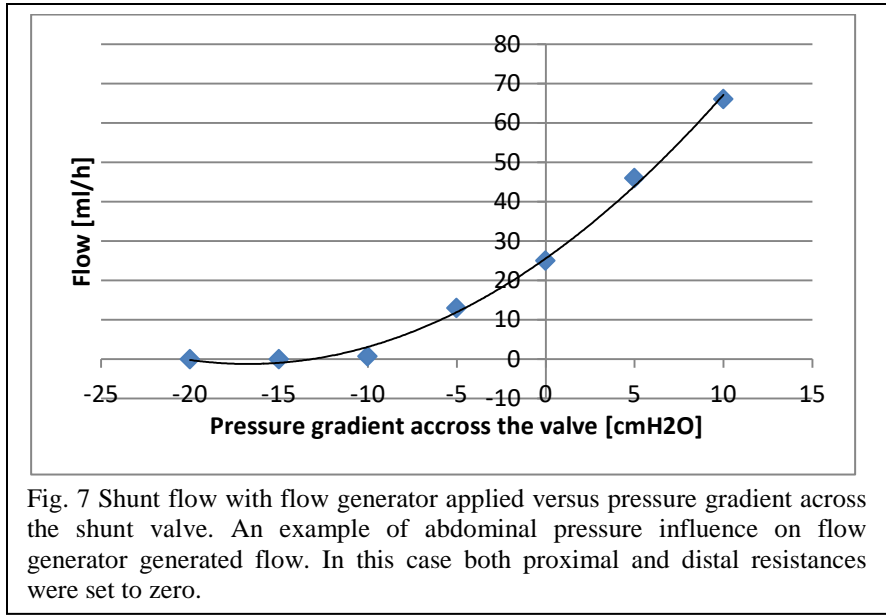
3.1.2 Abdominal pressure influence

Abdominal pressure shows a strong



The system seems to be more sensitive to proximal resistance in the low resistance region (0- 2 mmHg/ml/h). For the patent system, the flow rate is several times higher than for any non-zero combination of proximal and distal resistances. In the region of high resistances of 2-4 mmHg/ml/h, flow generator flow drops to

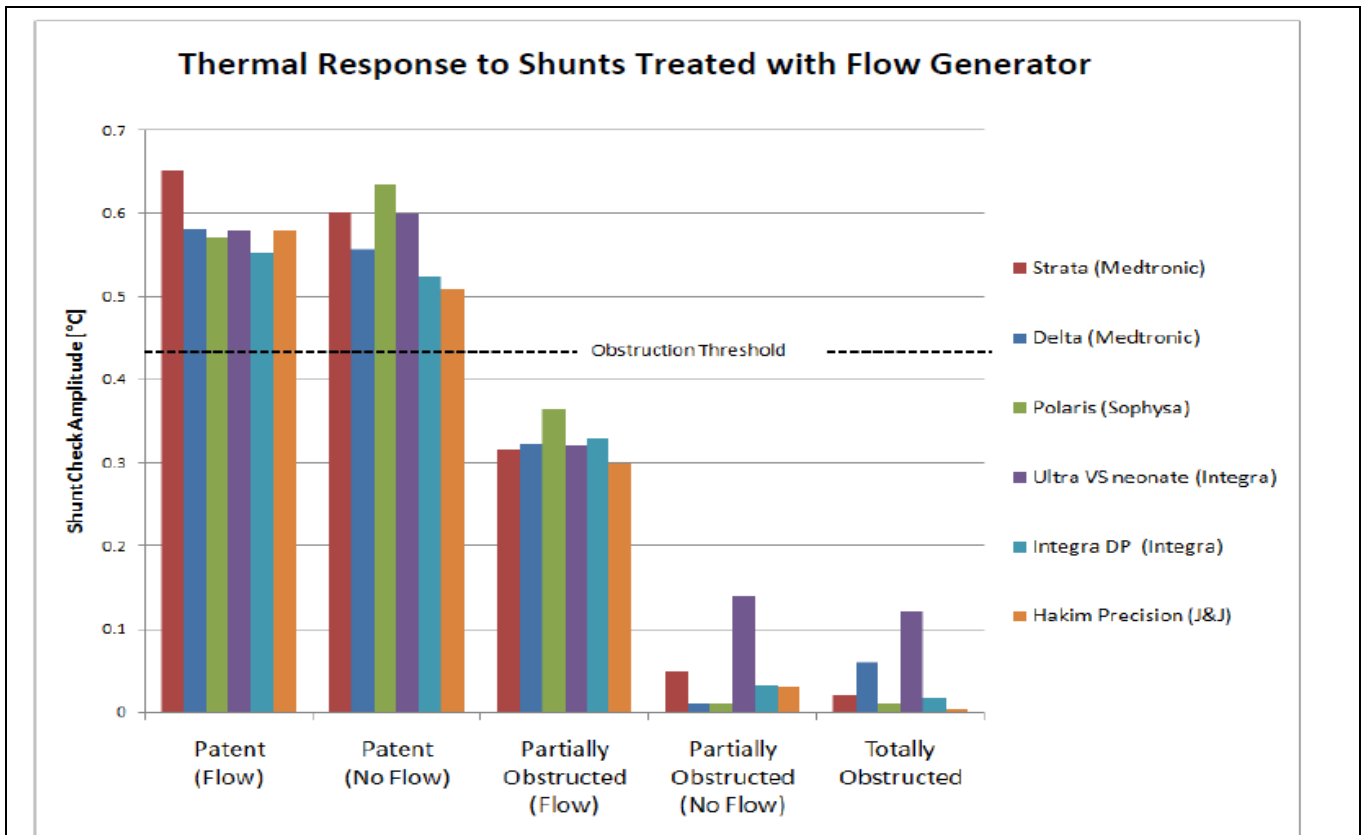
monotonic relationship with flow generator flow (see figure 7). Flow rate drops sharply with increasing abdominal pressure. From the data we gathered, it is evident that typically the flow generator flow rate is stopped if the abdominal pressure exceeds intracranial pressure by more than 5 cmH₂O .



3.2. Hypothesis 2. The combined flow generator plus the thermal CSF flow detection method can reliably differentiate between patent flow and

partially occluded flow.

Results are shown in figure 8. Clear differentiation is visible between patent and



partially occluded shunts. Completely occluded shunts show even lower thermal response to flow generation. Partial proximal obstruction was tested using resistance of 4 mmHg/ml/h.

ventricular tip of the catheter reflect the high hydraulic resistance caused by high velocity flow in the catheter. Strong pressure changes inside the dome are damped down to very

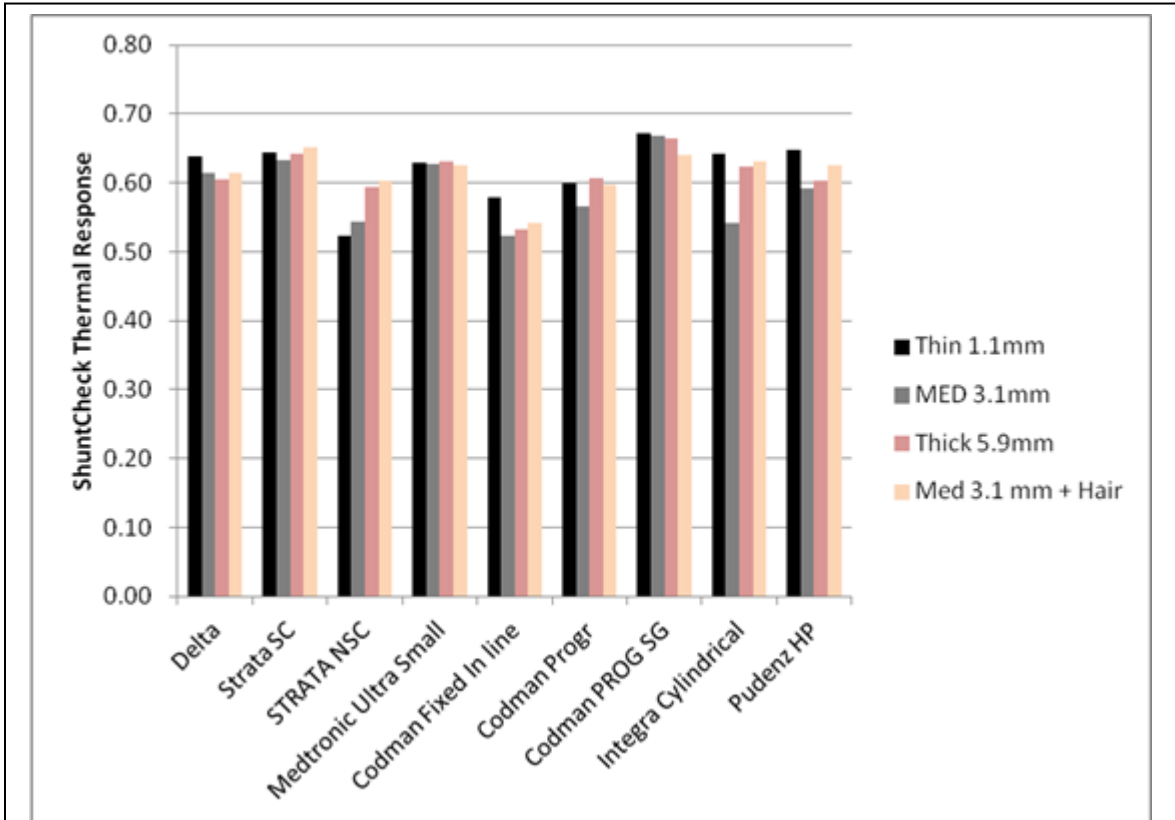


Fig.9 skin thickness and hair influence. Skin thickness simulated by Syndaver skin

Figure 9. shows thermal response variability caused by different skin thickness (SynDaver) and hair. Data was collected for 9 types of patent valves. Thermal responses vary by less than 0.18 °C with all temperature drops above 0.5 °C.

3.3. Safety.

Hypothesis 3. Vibrational flow generation is safe –it generates limited CSF drainage, does not generate strong ventricular and does not damage valves nor change the setting of programmable valves.

Pressure generated by the flow generator inside the dome and at the ventricular tip are shown in figure 10. Pressures recorded during flow generation inside the dome and at the

modest levels at the ventricular tip by the hydraulic resistance of the ventricular catheter. In the example in Figure 10, the dome peak-to-peak pressure is tenfold higher than the catheter tip peak-to-peak.

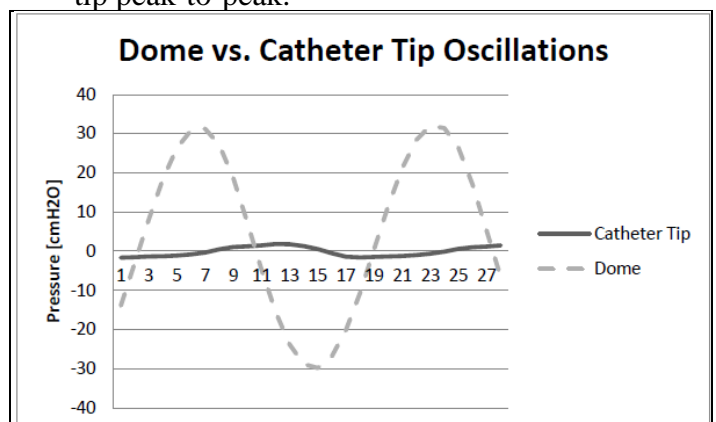


Figure 10 An example of a typical pressure waveform recorded inside the dome (dashed) and at the tip of catheter.

We tested several programmable valves and checked opening pressures and check valve action (we checked for possible back flows, due to valve damage) prior to and after flow generation testing. The opening pressure and check-valve action were not affected by the flow generator. During our extensive testing (for some valves the cumulative flow generation time was in order of several hours and more than hundred procedures per valve), we never observed a valve malfunction.

4. Conclusions

CSF flow intermittency limits the accuracy and clinical utility of all flow based methods for assessing shunt function. Promising results shown in this paper suggest that the flow generator can be combined with flow based methods, including the thermal CSF flow detector, to provide better shunt patency assessment than flow based methods alone. The combination of a flow generator and a thermal flow meter seems to be an inexpensive, safe and

reliable alternative to all existing techniques including radionuclide and MRI modalities. Our initial data suggest that this method could serve not only as a proximal resistance measurement but also, as a distal resistance assessment, especially when the abdominal pressure is kept at the low level (no more than 5cmH₂O above the intracranial pressure). The simplest way of applying this method would be a "total obstruction level assessment" since the flow generated by the flow generator drops as a function of total resistance (proximal and distal) (see figure 6). The vibrational flow generation effect is based on a solid mechanism, which is not compromised by a wide range of proximal and distal resistances. The method works even with relatively thick scalps and hair. We tested most types of popular valves and obtained relatively consistent results. We think that the method is ready for its clinical debut and should be tested on a population of symptomatic and asymptomatic patients in order to show its clinical usefulness.

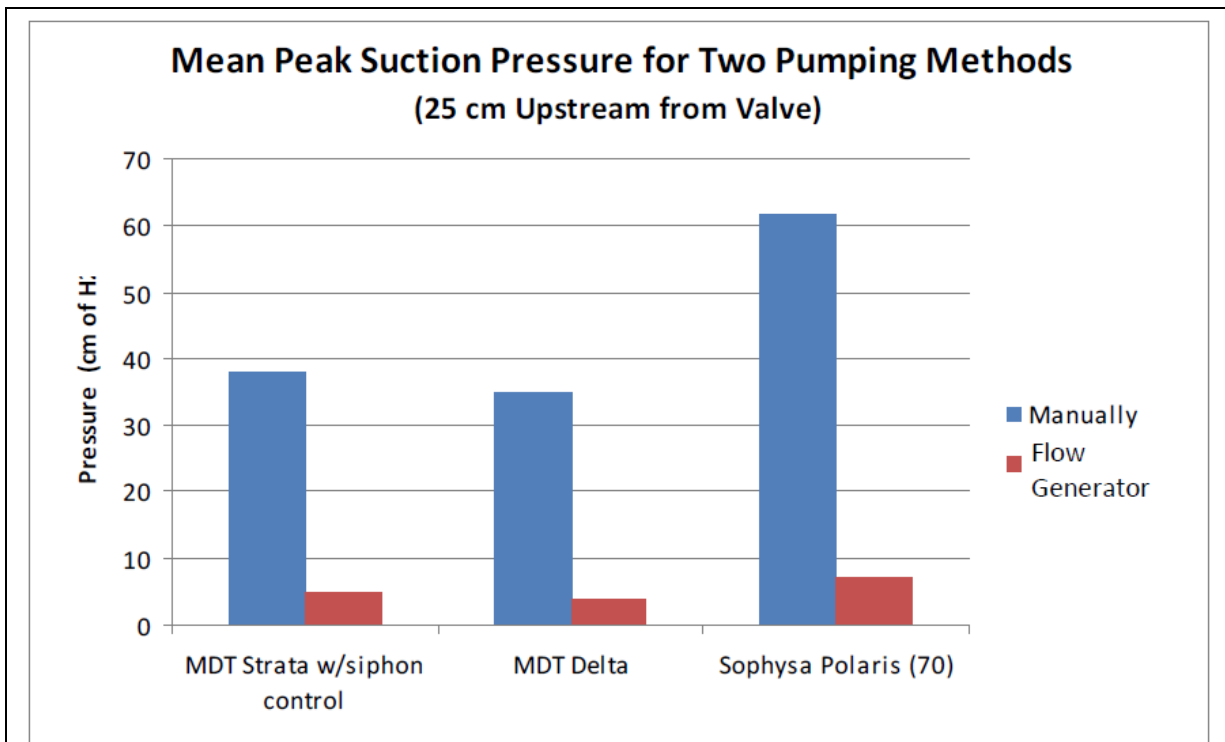


Fig.11. An example of a typical pressures measured at the ventricular tip of the catheter. Manual pumping shows greater suction generated inside the ventricle.

The proximal catheter adds a significant amount of resistance and pressure damping between the dome and the ventricular end of the catheter. This is caused by high flow rates (higher the flow rates, the higher the resistance) This is key to flow generator's safety and efficacy. The strong pressures generated in the dome reliably open and close the shunt valve and generate robust flow through the valve but at the same time the small suction pressure generated at the ventricular tip is 10 fold lower than suction generated by manual shunt pumping (see Figure 11).

5. References

1. Bondurant, C. and D. Jiminez, *Epidemiology of cerebrospinal fluid shunting*. *Pediatr Neurosurg*, 1995. **23**: p. 254-258.
2. Drake, J., et al., *Randomized trial of cerebrospinal fluid shunt valve design in pediatric hydrocephalus*. *Neurosurgery*, 1998. **43**: p. 294-305.
3. 16. Kestle, J., et al., *Lack of benefit of endoscopic ventriculoperitoneal shunt insertion: a multicenter randomized trial*. *J Neurosurg*, 2003. **98**: p. 284-290.
4. McGirt, M., et al., *Shunt survival and etiology of failures*. *Pediatr Neurosurg*, 2002. **36**: p. 248-255.
5. Zorc, J., et al., *Radiographic evaluation for suspected cerebrospinal fluid shunt obstruction*. *Pediatr Emerg Care*, 2002. **18**: p. 337-340.
6. Collins, P., A. Hockley, and D. Woollam, *Surface ultrastructure of tissues occluding ventricular catheters*. *J Neurosurg*, 1978. **48**: p. 609-613.
7. 19. Sainte-Rose, C., *Shunt obstruction: A preventable complication?* *Pediatr Neurosurg*, 1993. **19**: p. 156-164.
8. 20. Ventureyra, E. and M. Higgins, *A new ventricular catheter for the prevention and treatment of proximal obstruction in cerebrospinal fluid shunts*. *Neurosurgery*, 1994. **34**: p. 924-926.
9. Iskandar, B., et al., *Pitfalls in the diagnosis of ventricular shunt dysfunction: radiology reports and ventricular size*. *Pediatrics*, 1998. **101**: p. 1031-1036.
10. Frank E, Buonocore M, Hein L. *Magnetic resonance imaging analysis of extremely slow flow in a model shunt system*. *Child Nerv Syst* 8:73–75, 1991
11. Thermal dilution device 510(k) premarket notification K080168. http://www.accessdata.fda.gov/cdrh_docs/pdf8/K080168.pdf
12. Madsen, J. et al., *Evaluation of the Thermal dilution device Noninvasive Thermal Technique for Shunt Flow Detection in Hydrocephalus Patients*. *Neurosurgery* 68:198-205, 2011
13. Hidaka M, Matsumae M, Kaoru I. Tsugane R. Saito I, 1995. *Dynamic measurement of the flow rate in cerebrospinal fluid shunts in hydrocephalic patients*. *Eur. J. Nucl. Med.* 28: 888-893.
14. Martin AJ, Drake JM, Lemaire C, Henkelman RM. *Cerebrospinal fluid shunts: flow measurements with MKR imaging*. *Radiology* 173:243-247, 1989
15. Hori H, Moretti G, Rebora A, Crovato F: *The thickness of human of human scalp: normal and bald*. *The Journal of Investigative Dermatology* 1972; Vol 58 No 6, 396-399
16. Lupin AJ, Gardiner RJ: *Scalp thickness in the temporal region : its relevance to the development of cochlear implants*. *Cochlear Implants International* 2001; 2(1), 30-38.
17. Jay O, Havenith G: *Skin cooling on contact with cold materials: The effect of Blood flow during short term exposure*. *The Annals of Occupational Hygiene* 2004, Vol 48. No 2, 129-137
18. Hodges PW, Gandevia SC: *Changes in intra-abdominal pressure during postural and respiratory activation of the human*

- diaphragm*. Journal of Applied Physiology
2000, 89: 967-976
19. Gisolf J, van Lieshout JJ, van Heusden K, et al. : *Human cerebral venous outflow pathway depends on posture and central venous pressure*. Journal of Physiology, 2004, 317-327
 20. P. Hodges , S Gandevia Changes in intra-abdominal pressure during postural and respiratory activation of the human diaphragm. Journal of Applied Physiology 89: 967-976, 2000
 21. R. Daugherty, Joseph B Franzini Fluid Mechanics with Engineering applications McGraw -Hill Company New York 1977. p 212
 22. G. Cinalli W.J. Maixner, C. Sainte-Rose, Pediatric Hydrocephalus, Springer Milano 2004.pp 52.
 23. Thermal dilution device 510(k) application

Corresponding author: Marek Swoboda
Address: 324B Wall St
Princeton NJ 08540
USA
phone: 215 421 3121
email: dr.marekswoboda@gmail.com